

Bifurcations of electronic Rydberg wavepackets and core scattering

To cite this article: M W Beims and G Alber 1996 *J. Phys. B: At. Mol. Opt. Phys.* **29** 4139

View the [article online](#) for updates and enhancements.

You may also like

- [Trilobites, butterflies, and other exotic specimens of long-range Rydberg molecules](#)
Matthew T Eiles
- [Nondispersing radial Rydberg wavepackets in doubly core-driven two-electron atoms](#)
Birgit S Mecking and P Lambropoulos
- [Probing and manipulating high- \$n\$ near-circular Rydberg wave packets](#)
B Wyker, S Ye, F B Dunning et al.

Bifurcations of electronic Rydberg wavepackets and core scattering

M W Beims[†] and G Alber[‡]

[†] Instituto de Física, Universidade Federal do Rio Grande do Sul, 91501-970 Porto Alegre, Brazil

[‡] Theoretische Quantendynamik, Fakultät für Physik, Albert-Ludwigs-Universität, D-79104 Freiburg i. Brsg., Germany

Received 4 April 1996

Abstract. The influence of core scattering effects on the dynamics of a bifurcating electronic Rydberg wavepacket is investigated in the diamagnetic Kepler problem. Results are presented for a spherically symmetric nonhydrogenic core with particular emphasis on nongeneric bifurcations of the Edmonds–Garton–Tomkins orbit.

1. Introduction

Due to their large extension in comparison with the Bohr radius, Rydberg systems are well suited for the controlled preparation of spatially localized electronic wavepackets by laser fields. Recently studies on their time evolution have received considerable attention as such an electronic Rydberg wavepacket represents a quantum state which is close to the classical limit [1]. Its dynamics is dominated by the $(-1/r)$ Coulomb potential of the core which is formed by the nucleus and the residual electrons of the Rydberg system and which has a typical extension of a few Bohr radii. If an electronic Rydberg wavepacket penetrates the core it is scattered elastically or inelastically. This scattering can be characterized by a few quantum defect parameters which are a slowly varying function of energy close to a photoionization threshold. The dynamics of an electronic Rydberg wavepacket is particularly interesting in cases where the electrostatic core potential is modified at large distances by an external field so that the corresponding classical motion is not integrable. The paradigm in this respect is the diamagnetic Kepler problem [2–6].

In a case where the dynamics outside the core region is not integrable classically, the dynamics of electronic Rydberg wavepackets can be described theoretically in a convenient way by combining methods of quantum defect theory as far as the core dynamics is concerned with semiclassical methods which are capable of describing the dynamical aspects outside the core region [7]. Relevant quantum mechanical transition amplitudes can then be represented as a sum of contributions which are associated with all closed orbits of a Rydberg electron which start from and return again to the nucleus. Two extreme dynamical regimes can be distinguished.

(i) If the dynamics of the Rydberg electron outside the core region is determined completely by the $(-1/r)$ Coulomb potential, the quantum mechanical amplitudes of all these closed orbits interfere constructively. In this case scattering processes inside the core are significant as all closed orbits are scattered among each other and interfere constructively.

(ii) If the classical dynamics of the Rydberg electron outside the core region is not integrable classically, typically the contributing closed classical orbits are isolated [7–9]. In this case scattering processes inside the core lead to scatterings between these isolated closed orbits [7, 10, 11]. However, besides these scattered contributions there are also unscattered contributions to the relevant amplitudes. It has been pointed out in [7] and in a recent investigation [10] that scattered and unscattered contributions exhibit a different scaling behaviour with respect to the relevant semiclassical parameter \hbar . In particular, in the extreme semiclassical limit, i.e. $\hbar \rightarrow 0$, the scattered contributions become negligibly small in comparison with the unscattered ones.

Besides these two extreme dynamical regimes, an intermediate situation can be realized if an electronic Rydberg wavepacket is excited in an energy region where the relevant closed classical trajectories bifurcate [12–14]. In this case some of the relevant closed orbits approach each other and are no longer isolated. Thus strong quantum mechanical interference effects between the associated probability amplitudes take place. In particular, these interferences affect the \hbar -dependence of the quantum mechanical probability amplitudes. Thus in this case core effects are expected to be more significant than in the situation of isolated closed orbits.

In this paper the influence of core scattering effects on the dynamics of a bifurcating electronic Rydberg wavepacket is investigated. Generalizing recently developed uniform semiclassical methods [12] it is shown that core scattering processes can be taken into account in a straightforward way within a uniform semiclassical framework. Our discussion will focus on the diamagnetic Kepler problem which is a paradigm for a quantum system which can be studied in the laboratory and whose classical dynamics is not integrable. In particular, our discussion will concentrate on an ungeneric bifurcation of period four of the Edmonds–Garton–Tomkins orbit. This orbit extends along a straight line through the nucleus in the symmetry plane perpendicular to the applied static magnetic field. Due to the location in the symmetry plane this orbit exhibits a bifurcation phenomenon of the butterfly type. The high order of this bifurcation phenomenon implies strong quantum mechanical interferences between the relevant probability amplitudes of the closed orbits. Thus effects of core scattering are expected to be particularly significant in this case.

The paper is organized as follows. In section 2 basic results on the semiclassical description of the dynamics of an electronic Rydberg wavepacket are summarized and generalized to include core scattering effects. In section 3 a uniform semiclassical path representation is derived in which effects of core scattering in the presence of bifurcation phenomena are taken into account. Motivated by recent time-resolved studies of the diamagnetic Kepler problem [15, 16], elastic scattering of an electronic Rydberg wavepacket by a spherically symmetric ionic core is discussed in detail with particular emphasis on bifurcations of the Edmonds–Garton–Tomkins orbit.

2. Semiclassical treatment of wavepacket dynamics

In this section, previously developed semiclassical methods [1, 7] for describing the dynamics of laser-excited electronic Rydberg wavepackets in external, homogeneous, static magnetic fields are summarized briefly and generalized to include core scattering effects. In the following Hartree atomic units will be used with $e = \hbar = m_e = 1$.

Time-resolved pump–probe spectroscopy is a useful experimental technique for investigating the dynamics of an electronic Rydberg wavepacket [15, 16]. Typically, a

first, weak laser pulse with electric field strength

$$\mathbf{E}_1(t) = \mathcal{E}_1(t)\mathbf{e}_1 e^{-i\omega_1 t} + \text{CC} \quad (1)$$

whose pulse envelope is centred around time t_1 with pulse duration τ_1 prepares an electronic Rydberg wavepacket at time t_1 by exciting an atom from an initial state $|g\rangle$ of energy ϵ_g . The dynamics of this wavepacket is probed at a later time t_2 by another short and weak laser pulse $\mathbf{E}_2(t)$ (frequency ω_2 , pulse envelope $\mathcal{E}_2(t)$ and polarization \mathbf{e}_2) which induces a transition to a final state $|f\rangle$ of energy ϵ_f . The main theoretical problem in the description of such a pump–probe excitation process is the determination of the two-photon transition amplitude [1]

$$T_{fg}(\epsilon) = \langle f | \mathbf{d} \cdot \mathbf{e}_2^* (\epsilon + i0 - H)^{-1} \mathbf{d} \cdot \mathbf{e}_1 | g \rangle \quad (2)$$

in which the dynamics of the excited Rydberg electron in the absence of a pump and probe pulse is described by the Hamiltonian H . The atomic dipole operator is denoted \mathbf{d} . In terms of this quantity the experimentally observed pump–probe transition probability is given by

$$P_{g \rightarrow f} = \left| \frac{1}{2\pi} \int_{-\infty}^{\infty} d\epsilon e^{-i\epsilon(t_2-t_1)} T_{fg}(\epsilon) \tilde{\mathcal{E}}_1(\epsilon - \bar{\epsilon}) \tilde{\mathcal{E}}_2^*(\epsilon - \bar{\epsilon}) \right|^2 \quad (3)$$

with the Fourier transforms of the pulse envelopes denoted $\tilde{\mathcal{E}}_i(\epsilon) = \int_{-\infty}^{\infty} dt e^{i\epsilon t} \mathcal{E}_i(t + t_i)$, ($k = 1, 2$). For the sake of simplicity it has been assumed that $\bar{\epsilon} \equiv \epsilon_g + \omega_1 = \epsilon_f + \omega_2$.

The two-photon transition amplitude of equation (2) can be evaluated conveniently from the solution of the inhomogeneous Schrödinger equation [1, 17]

$$(\epsilon - H + i0) | F_\epsilon \rangle = \mathbf{d} \cdot \mathbf{e}_1 | g \rangle, \quad (4)$$

and the relation

$$T_{fg}(\epsilon) = \langle f | \mathbf{d} \cdot \mathbf{e}_2^* | F_\epsilon \rangle. \quad (5)$$

In the energy region close to a photonionization threshold the solution of equation (4) is simplified considerably by noting that three characteristic spatial regimes may be distinguished as far as the dynamics of an excited Rydberg electron is concerned [18, 19], namely

- (i) the core region ($0 \leq r \leq r_c \approx 1$) in which the dynamics of the Rydberg electron is dominated by electron correlation effects,
- (ii) the Coulomb region ($r_c \leq r \leq r_a$) in which the $(-1/r)$ Coulomb potential of the positively charged ionic core prevails and
- (iii) the asymptotic region ($1 \ll r_a \leq r$) in which any applied external electromagnetic field is at least as important as the Coulomb potential of the ionic core.

The (global) solution of equation (4) with the appropriate boundary condition can be constructed by patching together two local solutions of equation (4) which are valid in the core and Coulomb region on the one hand and in the Coulomb and asymptotic region on the other hand. Furthermore, if the extension of the Coulomb region is large, i.e. $r_a \gg 1$, an approximate local solution, which is valid in the Coulomb and asymptotic region, can be determined semiclassically. Within this general approach it has been shown [1, 7] that the two-photon transition amplitude

$$T_{fg}(\epsilon) = T_{fg}^{(s)} + \sum_{lm} \mathcal{D}_{lm}^{(+)} \mathcal{A}_{lm}(\epsilon) \quad (6)$$

consists of a smooth part $T_{fg}^{(s)}$ which is a slowly varying function of energy across any photonionization threshold and a second part which is a rapidly oscillating function of

energy and which is determined by the implicit relation

$$\begin{aligned} \mathcal{A}_{lm}(\epsilon) = & \int_0^{2\pi} d\varphi \int_0^\pi d\theta \sin\theta Y_l^m(\theta, \varphi)^* (-1)^l \\ & \times \sum_j \sqrt{J(0, \theta_{0j}, \varphi_{0j})/|J(\tau_j, \theta_{0j}, \varphi_{0j})|} e^{i[2\sqrt{8r_s} + S_{\epsilon_{lm}}(\tau_j, \theta_{0j}, \varphi_{0j}) - (\mu_j^> + 3)\pi/2]} \\ & \times \sum_{l'm'} Y_{l'}^{m'}(\theta_{0j}, \varphi_{0j}) (-1)^{l'} \left[2i\pi \mathcal{D}_{l'm'}^{(-)} + \sum_{l''m''} \chi_{l'm''}^{l'm''} \mathcal{A}_{l''m''}(\epsilon) \right]. \end{aligned} \quad (7)$$

Here the laser-induced initial excitation and final de-excitation processes are characterized by the photoionization and recombination dipole matrix elements $\mathcal{D}_{lm}^{(-)}$ and $\mathcal{D}_{lm}^{(+)}$ [1, 19]. The excited channels are specified by the angular momentum quantum numbers (l, m) of the Rydberg electron. Their threshold energies are denoted ϵ_{lm} . These dipole matrix elements are smooth functions of energy across any threshold. Outside the core region the dynamics of the excited Rydberg electron is characterized by all classical trajectories j which start on a sphere of radius $r_s \approx 1$ ($r_c \leq r_s \ll r_a$) with initial energy $(\epsilon - \epsilon_{lm})$, initial angles $\theta_{0j}, \varphi_{0j}$, and a purely radial momentum. According to equation (7) it is the trajectories which return again to this sphere at later times τ_j at angles θ, φ which contribute to $\mathcal{A}_{lm}(\epsilon)$. Important dynamical properties entering equation (7) are the classical actions $S_{\epsilon_{lm}}(\tau_j, \theta_{0j}, \varphi_{0j})$ and Maslov indices $\mu_j^>$ [20] of these trajectories which are accumulated outside the sphere of radius r_s . The quantity

$$J(\tau_j, \theta_{0j}, \varphi_{0j}) = \left. \frac{dx \wedge dy \wedge dz}{d\tau \wedge d\theta_0 \wedge d\varphi_0} \right|_{(\tau_j, \theta_{0j}, \varphi_{0j})} \quad (8)$$

characterizes the local projection of the Lagrangian manifold, which is generated by this family of classical trajectories, onto the configuration space. Inside the core region the dynamics of the Rydberg electron is described by the scattering matrix $\chi_{l'm''}^{l'm''}$ which is a slowly varying function of energy across any photoionization threshold [19]. In equation (7) it has been assumed that energy differences $\Delta\epsilon$ of possible inelastic transitions are small in comparison with the atomic unit of energy, i.e. $\Delta\epsilon r_s^{3/2} \ll 1$.

In further simplifications of equation (7) two limiting dynamical cases may be distinguished.

(i) In the absence of an external electromagnetic field the dynamics of an excited Rydberg electron is dominated by the Coulomb potential of the ionic core for $r \geq r_c$. In this case the relevant classical trajectories of equation (7) are purely radial Kepler orbits of angular momentum zero whose classical actions are independent of the emission angles $(\theta_{0j}, \varphi_{0j})$. This implies that all contributions to equation (7) add coherently in phase. Thus in this special case equations (6) and (7) reduce to the well known result of multichannel quantum defect theory [1, 19]. In particular, in this case the dependence of $T_{fg}(\epsilon)$ on the matrix χ indicates that effects of scattering by the ionic core are significant and cannot be neglected.

(ii) Typically, in the presence of an external electromagnetic field $e^{iS_{\epsilon_{lm}}(\tau, \theta_0, \varphi_0)}$ is a rapidly oscillating function of the final angles (θ, φ) at which the classical trajectories return again to the sphere of radius r_s . Therefore, for low values of the angular momentum in equation (7) the integration over these final angles can be performed in the stationary phase approximation. Thus the dominant contributions originate from points of stationary phase which correspond to closed orbits which start from and return again to the Coulomb centre [7–9].

A paradigm of this second type of dynamical case is the diamagnetic Kepler problem

in which the dynamics of the excited Rydberg electron is described by the Hamiltonian [4]

$$H = H_A - \gamma L_z + \frac{1}{2} \gamma^2 r^2 \sin^2 \theta. \quad (9)$$

Here the atomic Hamiltonian H_A dominates the dynamics of the Rydberg electron in the core and Coulomb region where the influence of the external homogeneous, static magnetic field $\mathbf{B}(\mathbf{x}) = \gamma \mathbf{e}_z$ is negligible. The second and third terms on the right-hand side of equation (9) are the paramagnetic and diamagnetic interaction terms with γ denoting the magnetic field strength in atomic units. (The atomic unit of magnetic field strength is $B_0 = 4.71 \times 10^5$ T.) In the case of weak magnetic fields, i.e. $\gamma \ll 1$, and for energies close to the first photoionization threshold the presence of the diamagnetic interaction term in equation (9) implies that the dynamics of the Rydberg electron in the Coulomb and asymptotic region is not integrable classically.

In the evaluation of equation (7) one has to take into account that outside the core region the Hamiltonian H of equation (9) is axially symmetric around the magnetic field axis. Therefore the z -component of the angular momentum L_z is a conserved quantity. This implies that in equation (7) classical trajectories with different emission angles φ_{0j} interfere constructively so that within the framework of the stationary phase approximation the closed classical trajectories contributing to equation (7) can be isolated only with respect to the emission angle θ_{0j} . Thus solving equation (7) by iteration, a semiclassical path representation is obtained in which $T_{fg}(\epsilon)$ is represented as a sum of contributions which correspond to repeated returns of a Rydberg electron to the core region [7]. Assuming that all relevant closed orbits are well separated with respect to the emission angles θ_0 the first few terms of this semiclassical isolated-closed-orbit representation are given by

$$T_{fg}(\epsilon) = T_{fg}^{(s)} + 2i\pi \sum_{l,l',m} \mathcal{D}_{lm}^{(+)} \{t_{ll',m}^{(1)} \delta_{l'l''} + t_{ll',m}^{(2)} \delta_{l'l''} + t_{ll',m}^{(3)} \delta_{l'l''} + t_{ll',m}^{(1)} f_{l'l'';m}^{(1)} + t_{ll',m}^{(1)} f_{l'l'';m}^{(2)} + t_{ll',m}^{(2)} f_{l'l'';m}^{(1)} + \dots\} \mathcal{D}_{l''m}^{(-)} \quad (10)$$

with

$$t_{ll',m}^{(n)} = -i \sum_j (2\pi)^{3/2} Y_l^m(\theta_j, 0)^* (-1)^l [\sigma_j^{(n)}(\epsilon_m)]^{1/2} \times e^{[n(S_j(\epsilon_m) - m\pi v_j) - \mu_j^{(n)} \pi/2 + \pi/4]} Y_{l'}^m(\theta_{0j}, 0) (-1)^{l'} \quad (11)$$

and $\epsilon_m = \epsilon + m\gamma$. Equation (10) generalizes previously derived semiclassical results [7–9] in which the effects of core scattering have been neglected. The probability amplitude $t_{ll',m}^{(n)}$ characterizes the contribution of the Rydberg electron which is associated with its n th return to the core region without being scattered during its intermediate crossings of the core. The classical dynamics of the relevant isolated closed orbits j is characterized by their classical actions $nS_j(\epsilon_m)$, their number of crossings of the symmetry axis v_j and their Maslov indices $\mu_j^{(n)}$. The amplitude of the n th return of trajectory j is also determined by the classical cross section

$$\sigma_j^{(n)}(\epsilon) = \sin \theta_j \sin \theta_{0j} \left/ \left| \frac{\partial p_\theta}{\partial \theta_0} \frac{\sin n u_j}{\sin u_j} \right| \right. \quad (12)$$

Here θ_j denotes the final value of the return angle of the classical closed orbit j . The stability exponent of this closed orbit is denoted u_j and p_θ is the canonical momentum associated with θ . The cross section of equation (12) determines the range of initial emission angles, or equivalently the size of the characteristic Fresnel zone [21], within which orbits interfere constructively. For the sake of simplicity it has been assumed in equation (10) that inelastic scattering by the ionic core is negligible and that the core is spherically symmetric. Thus

the scattering matrix of the core is independent of the magnetic quantum number m and diagonal with respect to the angular momentum quantum number l , i.e. $\chi_{lm}^{l'm'} = \chi_l \delta_{ll'} \delta_{mm'}$. However, starting from equation (7) it is straightforward to generalize equation (10) to cases which involve more complicated core scattering processes. In equation (10) the influence of scattering by the ionic core is described by the terms involving the scattering amplitudes $f_l = \chi_l - 1$. As the ionic core, in which the electron correlation effects take place, has a typical extension of a few Bohr radii, f_l is nonzero only for low values of the angular momentum l . Scaling properties of the Hamiltonian of equation (9) imply that classical actions of relevant closed orbits are proportional to $\lambda = \gamma^{-1/3}$ (in units of \hbar) so that $\sigma_j^{(n)}(\epsilon) = O(\lambda^{-1})$. As has already been pointed out previously [7] this implies that unscattered contributions to equation (10) are of order $O(\lambda^{-1/2})$ whereas scattered contributions are of order $O(\lambda^{-1})$ and become vanishingly small in the semiclassical limit, $\lambda \gg 1$. At energies at which $\sin nu_j = 0$ the classical cross section $\sigma_j^{(n)}(\epsilon)$ tends to infinity indicating that a bifurcation phenomenon takes place and the relevant closed orbits can no longer be considered as being isolated. In such a case equation (10) is no longer valid and the integration over angles appearing in equation (7) has to be performed by using uniform semiclassical techniques [12]. The resulting strong quantum mechanical interference effects are expected to change the scaling behaviour of unscattered and scattered contributions so that scattered contributions might become more significant than in the isolated-closed-orbit case.

3. Bifurcation phenomena and core scattering

In order to investigate core scattering effects in the presence of bifurcation phenomena let us consider bifurcations of the Edmonds–Garton–Tomkins orbit in the diamagnetic Kepler problem in more detail.

The classical dynamics of bifurcations in the diamagnetic Kepler problem has been investigated in detail in [22]. It has been shown that due to the discrete reflection symmetry of the Hamiltonian H of equation (9) with respect to a plane through the Coulomb centre and perpendicular to the magnetic field axis the Edmonds–Garton–Tomkins orbit exhibits nongeneric bifurcation phenomena. This orbit starts from the atomic nucleus and extends along a straight line in the symmetry plane. Bifurcations of this particular orbit and their manifestation in the dynamics of an electronic Rydberg wavepacket in the absence of core scattering effects have already been discussed previously [12]. In figure 1 characteristics of the bifurcation of period four which occurs at energy $\epsilon_2 = -0.50191\gamma^{2/3}$ are summarized briefly. The classical phase space structure of this particular bifurcation phenomenon of period four, which has been termed ‘Pacman’, has been investigated in detail by Mao and Delos [22]. As apparent from the energy dependence of the emission angle θ_0 shown in figure 1(a), at energy $\epsilon_1 = -0.5037\gamma^{2/3}$ a stable and an unstable closed orbit (I_1, I_2) are created by a saddle-node bifurcation together with their symmetry-induced reflected counterparts (I_{-1}, I_{-2}). At energy ϵ_2 the stable orbits I_1 and I_{-1} coalesce with the Edmonds–Garton–Tomkins orbit I_0 so that for energies $\epsilon > \epsilon_2$ only the three closed orbits I_0 (stable) and I_2, I_{-2} (unstable) remain. The coalescence of the three stable closed orbits I_0, I_1, I_{-1} at energy ϵ_2 is an ungeneric bifurcation phenomenon of period four which is possible because of the discrete reflection symmetry of the Hamiltonian H in the Coulomb and asymptotic region. Similar bifurcation phenomena of periods seven and 18 take place at energies $\epsilon_3 = -0.4194\gamma^{2/3}$ and $\epsilon_4 = -0.4365\gamma^{2/3}$.

With the help of time-resolved pump–probe experiments of the type described in section 2 and by choosing the laser frequency so that $\bar{\epsilon} \approx \epsilon_1 \approx \epsilon_2$ the manifestation

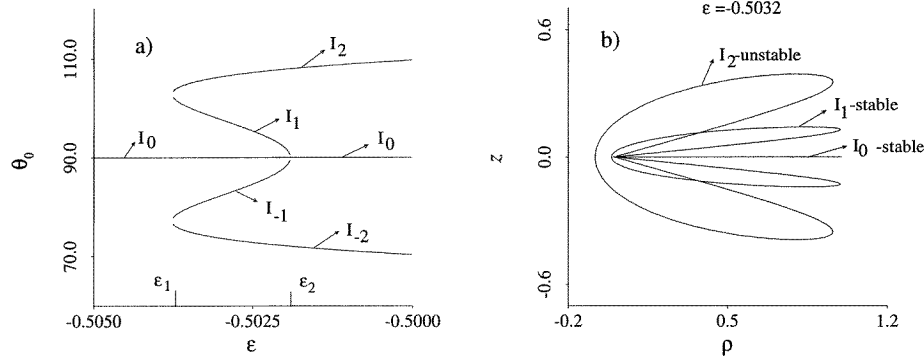


Figure 1. Emission angles θ_0 of orbits I_0 , $I_{\pm 1}$ and $I_{\pm 2}$ as a function of scaled energy $\tilde{\epsilon} = \epsilon/\gamma^{2/3}$ (a) and their form in configuration space with $\tilde{\rho} = \sqrt{x^2 + y^2}\gamma^{2/3}$ and $\tilde{z} = z\gamma^{2/3}$ (b).

of these classical bifurcation phenomena in the time evolution of an electronic Rydberg wavepacket can be investigated. Furthermore, by selecting the laser polarizations of pump and probe pulse perpendicular to the homogeneous, static magnetic field and restricting the observation times of interest, $t_2 - t_1$, to times of the order of a few multiples of the orbit time of the Edmonds–Garton–Tomkins orbit, T_0 , the corresponding pump–probe signal of equation (3) is dominated by the contributions arising from these five classical closed orbits [12]. For the theoretical description of core scattering in the presence of these bifurcation phenomena equation (10) has to be generalized and a uniform semiclassical description of the significantly contributing closed orbits I_0 , $I_{\pm 1}$, $I_{\pm 2}$ is needed. In the absence of core scattering a uniform semiclassical description has already been developed previously [12]. In particular, it has been shown that in equation (10) the contributions of the $2n$ th return of orbit I_0 and the n th return of orbits $I_{\pm 1}$, $I_{\pm 2}$ ($n \geq 1$) to the Coulomb centre can be described uniformly by the canonical comparison integral of a cuspidal butterfly catastrophe [23]

$$J_m^{(2n)}(\epsilon) = \int_{-\infty}^{\infty} d\theta_0 G_m^{(2n)}(\theta_0, \epsilon) e^{iF_m^{(2n)}(\theta_0, \epsilon)}. \quad (13)$$

In equation (13) it has been assumed that the main contribution to the integral over the emission angle θ_0 of the Rydberg electron comes from values $\theta_0 \approx \pi/2$ so that the limits of integration can be extended to infinity. The coefficients $A_{km}^{(2n)}(\epsilon)$ and $a_{km}^{(2n)}(\epsilon)$ of the polynomials

$$G_m^{(2n)}(\theta_0, \epsilon) = \sum_{k=0,1,2} A_{km}^{(2n)}(\epsilon)(\theta_0 - \pi/2)^{2k} \quad (14)$$

and

$$F_m^{(2n)}(\theta_0, \epsilon) = \sum_{k=0,1,2,3} a_{km}^{(2n)}(\epsilon)(\theta_0 - \pi/2)^{2k} \quad (15)$$

are smooth functions of energy across the energy range (ϵ_1, ϵ_2) . They are determined uniquely by the requirements that

(i) the stationary phase points of this comparison integral are identical with the emission angles of the relevant classical closed orbits and that

(ii) in the semiclassical limit, i.e. $\lambda = \gamma^{-1/3} \gg 1$, for energies sufficiently far away from the bifurcation energies ϵ_1 and ϵ_2 the stationary phase evaluation of $J_m^{(2n)}(\epsilon)$ reduces to the corresponding semiclassical result of the isolated-closed-orbit approximation of equation (10).

As has been shown in detail in [12], in the energy regime $\epsilon_1 < \epsilon < \epsilon_2$ the energy dependence of these coefficients can be determined by these requirements from the classical properties of the relevant five closed orbits $I_0, I_{\pm 1}, I_{\pm 2}$ and the corresponding photoionization and recombination dipole matrix elements. As these coefficients are slowly varying functions of energy they can be extrapolated beyond this energy regime by polynomial fits with respect to energy. By this approach the energy dependence of these coefficients has been determined in [12] for the above-mentioned bifurcation phenomena of period four, seven and 18.

In general, the canonical comparison integral of equation (13) has to be determined numerically. In the semiclassical limit, i.e. $\lambda \gg 1$, it is a rapidly oscillating function of the emission angle θ_0 so that it can be evaluated numerically in a convenient way with the help of the method of steepest descent [24]. Thereby the original contour of integration, which extends along the real axis in the complex θ_0 -plane, is deformed so that it goes through saddle points of $F_m^{(2n)}(\theta_0, \epsilon)$ along paths of steepest descent. Along this deformed integration contour the real part of $F_m^{(2n)}(\theta_0, \epsilon)$ remains constant so that the comparison integral is no longer oscillating rapidly. Typically the dominant contribution to the comparison integral comes from a small neighbourhood of these saddle points. The contributions from the saddle points which are not located on the real θ_0 -axis might be viewed as contributions from ghost orbits [25]. Physically speaking, contributions of these ghost orbits arise from classical trajectories which are almost closed. It should be mentioned that this numerical approach is more general than the saddle point method in which, in addition to the above-mentioned deformation of the integration contour, the exponent $F_m^{(2n)}(\theta_0, \epsilon)$ is approximated by a second-order Taylor expansion around each saddle point. In particular, this numerical steepest descent approach can be applied irrespective of whether the saddle points coalesce or are well separated.

Within this uniform semiclassical approximation the isolated-closed-orbit expression of equation (10) can be generalized in a straightforward way to the case of core scattering effects in the presence of bifurcation phenomena by replacing the diverging contributions of the coalescing closed orbits by the relevant canonical integral. Let us consider laser excitation of a Rydberg electron from an initially prepared energetically low lying bound state $|g\rangle$ with angular momentum zero in more detail. Let us also assume that the final state $|f\rangle$ is an s-state and that the polarizations of pump and probe pulses are equal and perpendicular to the magnetic field so that the possible magnetic quantum numbers of the excited Rydberg electron are given by $m = \pm 1$. This implies that the dominant contribution to the pump-probe transition probability of equation (3) originates from the orbits $I_0, I_{\pm 1}, I_{\pm 2}$, if the significantly excited energy range is concentrated around $\epsilon_1 \approx \epsilon_2$ and if the observation times of interest, i.e. $(t_2 - t_1)$, are of the order of the classical orbit time of the Edmonds-Garton-Tomkins orbit T_0 . Furthermore, for the sake of simplicity it will be assumed that the ionic core is spherically symmetric and that scattering phase shifts are negligible for angular momenta $l \geq 2$, i.e. $f_l = 0$ for $l \geq 2$. Therefore in this case only the scattering phase shift for $l = 1$ is relevant. Thus the first few terms of the uniform semiclassical path representation for the two-photon transition amplitude are given by

$$\begin{aligned}
 T_{fg}(\epsilon) = & T_{fg}^{(s)} + 2i\pi \sum_{m=\pm 1} \mathcal{D}_{1m}^{(+)} \{ t_{11;m}^{(1)} + J_m^{(2)}(\epsilon) + t_{11;m}^{(3)} + J_m^{(4)}(\epsilon) + t_{11;m}^{(1)} f_1 t_{11;m}^{(1)} \\
 & + J_m^{(2)}(\epsilon) f_1 t_{11;m}^{(1)} + t_{11;m}^{(1)} f_1 J_m^{(2)}(\epsilon) + t_{11;m}^{(1)} f_1 t_{11;m}^{(1)} f_1 t_{11;m}^{(1)} + t_{11;m}^{(1)} f_1 t_{11;m}^{(3)} \\
 & + t_{11;m}^{(3)} f_1 t_{11;m}^{(1)} + t_{11;m}^{(1)} f_1 J_m^{(2)}(\epsilon) f_1 t_{11;m}^{(1)} + J_m^{(2)}(\epsilon) f_1 t_{11;m}^{(1)} f_1 t_{11;m}^{(1)} \\
 & + t_{11;m}^{(1)} f_1 t_{11;m}^{(1)} f_1 J_m^{(2)}(\epsilon) + t_{11;m}^{(1)} f_1 t_{11;m}^{(1)} f_1 t_{11;m}^{(1)} f_1 t_{11;m}^{(1)} + \dots \} \mathcal{D}_{1m}^{(-)}. \quad (16)
 \end{aligned}$$

Equation (16) is one of the central results of this paper. The uniform canonical integral $J_m^{(2n)}(\epsilon)$ has the property that for $\lambda = \gamma^{-1/3} \gg 1$ and for energies $\epsilon_1 < \epsilon < \epsilon_2$ it reduces to those contributions of the amplitude $t_{11;m}^{(2n)}$ of equation (11) which arise from the classical closed orbits I_0 , $I_{\pm 1}$ and $I_{\pm 2}$. Inserting equation (16) into equation (3) yields the pump–probe transition probability with which the time evolution of an electronic Rydberg wavepacket can be investigated.

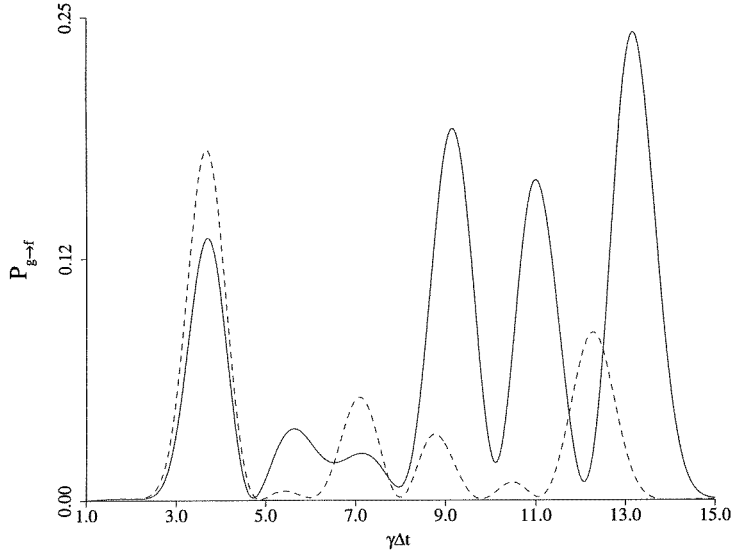


Figure 2. Pump–probe transition probability $P_{g \rightarrow f}(\Delta t)$ in units of $(2\pi \sum_{m=\pm 1} |\mathcal{D}_{1m}^{(+)} \mathcal{E}_2^* \mathcal{D}_{1m}^{(-)} \mathcal{E}_1| \times \tau_1 \tau_2)^2$ with $\bar{\epsilon} = \epsilon_g + \omega_1 = \epsilon_f + \omega_2 = -0.49\gamma^{2/3}$, $\gamma = 5 \times 10^{-6}$ ($\equiv 2.36$ T), $\tau_1 = \tau_2 = 0.04/\gamma$, and $\alpha_1 = 0.66$ (full curve). The broken curve shows the corresponding result for $\alpha_1 = 0$.

In figure 2 the pump–probe transition probability $P_{g \rightarrow f}(\Delta t)$ is shown as a function of the time delay $\Delta t = t_2 - t_1$ between pump and probe pulse. The magnetic field strength is $\gamma = 5 \times 10^{-6}$ which implies $\lambda = \gamma^{-1/3} \approx 100$ so that the semiclassical approximation is expected to be valid. The quantum defect of the excited Rydberg states with angular momentum $l = 1$ is the same as for the rubidium atom, namely $\alpha_1 = 0.66$. The laser polarizations are chosen perpendicular to the applied magnetic field and the mean excited energy and the pulse durations of pump and probe pulse are chosen so that for time delays Δt of the order of a few multiples of $T_0 \approx 1.8/\gamma = 8$ ps the dynamics of the electronic Rydberg wavepacket is dominated by the five closed, classical orbits I_0 , $I_{\pm 1}$ and $I_{\pm 2}$ and their bifurcations. The recombination peaks of figure 2 at multiples of T_0 are associated with subsequent returns of the excited electronic Rydberg wavepacket along orbit I_0 . The first significant peak in figure 2 appears at $\Delta t \approx 2T_0$. In comparison with this recombination peak the contribution of the first return along orbit I_0 is negligible. The magnitude of this maximum is determined by

(i) the strong quantum mechanical interference effects between the contributions of the second return of orbit I_0 and the first returns of orbits $I_{\pm 1}$ and $I_{\pm 2}$ which are described by $J_m^{(2)}(\epsilon)$ in equation (16) and

(ii) the fraction of the Rydberg wavepacket which has been scattered after its first return to the core region and returns along orbit I_0 again at time $2T_0$. This latter process is described by the first term in the third line of equation (16).

Comparison with the broken curve in figure 2, in which the corresponding result is shown for $\alpha_1 = 0$ (i.e. in the absence of core scattering processes), demonstrates that these two contributions interfere destructively. The second maximum of figure 2 which appears at $\Delta t \approx 5.4/\gamma$ originates from the third return of a fraction of the excited electronic wavepacket along orbit I_0 with zero, one or two intermediate scatterings of the Rydberg electron by the ionic core. Due to the bifurcation between orbits I_0 , $I_{\pm 1}$ and $I_{\pm 2}$ the contribution which involves one intermediate scattering is large. This can be seen again by comparison with the broken curve. Similarly all subsequent maxima appearing in figure 2 can be interpreted in a straightforward way on the basis of the uniform semiclassical path representation of equation (16). In particular, the large maximum at $\Delta t \approx 13/\gamma$ is due to a bifurcation of period seven of the Edmonds–Garton–Tomkins orbit which has been mentioned above and has been discussed in detail in [12].

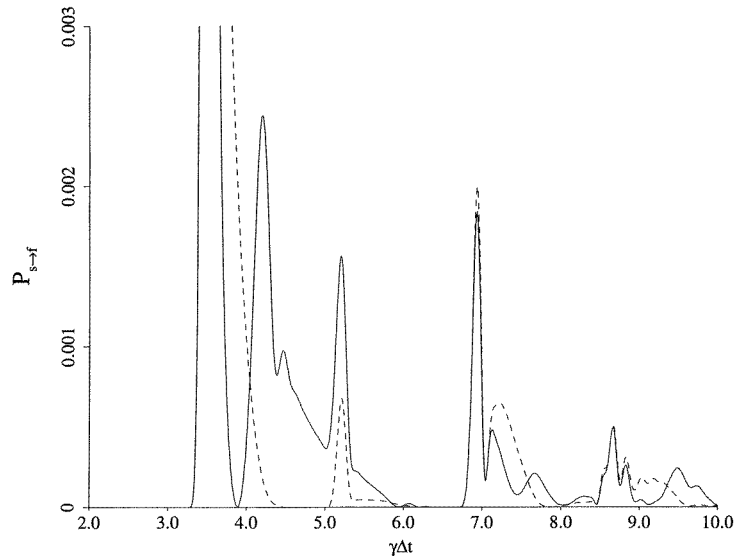


Figure 3. Pump–probe transition probability $P_{g \rightarrow f}(\Delta t)$ in units of $(2\pi \sum_{m=\pm 1} |\mathcal{D}_{1m}^{(+)} \mathcal{E}_2^* \mathcal{D}_{1m}^{(-)} \mathcal{E}_1| \times \tau_1 \tau_2)^2$ for a window resonance with $\bar{\epsilon} = \epsilon_g + \omega_1 = \epsilon_f + \omega_2 = -0.5\gamma^{2/3}$, $\gamma = 10^{-9}$ ($\equiv 0.471$ mT), $\tau_1 = \tau_2 = 0.04/\gamma$, $\alpha_1 = 0.5$, $\epsilon_p = -0.5025\gamma^{2/3}$, $\Gamma_p = \gamma$.

Additional interesting effects arise if the laser-excited Rydberg series is perturbed by channel coupling. In figure 3 a model problem involving an isolated perturber is investigated in more detail. The resulting time dependence of the pump–probe transition probability $P_{g \rightarrow f}(\Delta t)$ is depicted by the full curve. Again, as in figure 2, the laser polarizations of pump and probe pulse are perpendicular to the magnetic field axis and the quantum defects for angular momentum states with $l \geq 2$ are assumed to be vanishingly small. The excited energy range and the observation times of interest are chosen so that the dominant contribution comes from the five closed orbits I_0 , $I_{\pm 1}$, $I_{\pm 2}$. The isolated perturber is assumed to be located in the energy range in which all these five closed orbits exist. Furthermore, its width Γ_p is assumed to be so small that it is equal to the Larmor angular velocity of the Rydberg electron in the applied static magnetic field, i.e. $\Gamma_p = \gamma$. Its mixing into the excited Rydberg states with angular momentum $l = 1$ leads to an energy dependence of the

quantum defect of the form [19]

$$\alpha_1(\epsilon) = \alpha_1 - \frac{1}{\pi} \arctan\left(\frac{\Gamma_P/2}{\epsilon - \epsilon_P}\right). \quad (17)$$

If this perturber is not coupled directly to the initial and final states $|g\rangle$ and $|f\rangle$ by pump and probe pulses, it gives rise to a window resonance. The energy dependence of the quantum defect $\alpha_1(\epsilon)$ implies an additional energy dependence of the photoionization and recombination dipole matrix elements and of the scattering amplitude $f_1 = e^{2i\pi\alpha_1(\epsilon)} - 1$ of equation (16). According to equation (3) this additional energy dependence leads to time delays in the time evolution of the laser-excited electronic Rydberg wavepacket. In figure 3 the effects of these time delays on the pump–probe transition probability are investigated for such a window resonance. The corresponding time dependence in the absence of a window resonance is depicted by the broken curve. The first maximum of the broken curve shows the contribution of the second return of orbit I_0 and the first return of orbits $I_{\pm 1}$ and $I_{\pm 2}$ which are described by $J_m^{(2)}(\epsilon)$ in equation (16). Effects which are caused by the time delays resulting from the energy-dependent quantum defect of equation (17) are apparent from the full curve in figure 3. In particular, the time delays of the contributions associated with the first returns of orbits $I_{\pm 1}$ and $I_{\pm 2}$ are so significant that these contributions overlap with the corresponding amplitude of the third return of orbit I_0 which is centred around $\Delta t \approx 5.2/\gamma$. The constructive interference between these contributions is clearly visible.

In conclusion, it has been shown that the influence of core scattering on the dynamics of an electronic Rydberg wavepacket can be described in a convenient way with the help of quantum defect theory and semiclassical methods. The connection between quantum dynamics and the corresponding classical motion is then exhibited quantitatively. In cases where the corresponding classical dynamics is dominated by bifurcation phenomena, uniform semiclassical methods have to be used for a satisfactory theoretical description. In the case of the diamagnetic Kepler problem it has been shown that the effects of core scattering can be enhanced significantly in the presence of bifurcation phenomena. Furthermore, core scattering processes do not only lead to the appearance of additional recombination peaks in time resolved studies of wavepacket dynamics but they can also lead to significant time delays, in particular if they are due to channel couplings involving perturbers with lifetimes of the order of the inverse Larmor frequency.

Acknowledgments

This work is supported by the Deutsche Forschungsgemeinschaft (SFB 276) and the EC-Human Capital and Mobility Contract ERBCHRXCT940552. One of us (MWB) also wishes to acknowledge financial support by the Deutscher Akademischer Austauschdienst and the Fundação de Amparo a Pesquisa do Rio Grande do Sul.

References

- [1] Alber G and Zoller P 1991 *Phys. Rep.* **199** 231
- [2] Holle A, Wiebusch G, Main J, Hager B, Rottke H and Welge K H 1986 *Phys. Rev. Lett.* **56** 2594
Holle A, Main J, Wiebusch G, Rottke H and Welge K H 1988 *Phys. Rev. Lett.* **61** 161
- [3] Welch G R, Kash M M, Iu C, Hsu L and Kleppner D 1989 *Phys. Rev. Lett.* **62** 893
Iu C, Welch G R, Kash M M, Hsu L and Kleppner D *Phys. Rev. Lett.* **63** 1133
- [4] Friedrich H and Wintgen D 1989 *Phys. Rep.* **183** 37 and references therein
- [5] Delande D, Bommier A and Gay J C 1991 *Phys. Rev. Lett.* **66** 141
- [6] Tanner G, Hansen K T and Main J 1996 *Nonlinearity* submitted

- [7] Alber G 1989 *Z. Phys. D* **14** 307
- [8] Bogomolny E B 1988 *Pis. Zh. Eksp. Teor. Fiz.* **47** 445 (Engl. transl. 1988 *JETP Lett.* **47** 526)
- [9] Du M L and Delos J B 1988 *Phys. Rev. A* **38** 1896; 1913
- [10] Dando P A, Monteiro T S, Delande D and Taylor K T 1995 *Phys. Rev. Lett.* **74** 1099
- [11] Hüpper B, Main J and Wunner G 1995 *Phys. Rev. Lett.* **74** 2650
- [12] Beims M W and Alber G 1993 *Phys. Rev. A* **48** 3123
- [13] Peters A D, Jaffé C and Delos J B 1994 *Phys. Rev. Lett.* **73** 2825
- [14] Main J, Wiebusch G, Welge K H, Shaw J and Delos J B 1994 *Phys. Rev. A* **49** 847
- [15] Marmet L, Held H, Raithel G, Yeazell J A and Walther H 1994 *Phys. Rev. Lett.* **72** 3779
- [16] Wals J, Fielding H H, Christian J F, Snoek L C, van der Zande W J and van Linden van den Heuvell H B 1994 *Phys. Rev. Lett.* **72** 3783
- [17] Dalgarno A and Lewis J T 1955 *Proc. R. Soc. A* **233** 70
- [18] Fano U and Rau A R P 1986 *Atomic Collisions and Spectra* (New York: Academic)
- [19] Seaton M J 1983 *Rep. Prog. Phys.* **46** 167
- [20] Maslov V P and Fedoriuk M V 1981 *Semiclassical Approximation in Quantum Mechanics* (Boston, MA: Reidel)
- [21] Kravtsov Yu A and Orlov Yu I 1990 *Geometrical Optics of Inhomogeneous Media* (Berlin: Springer)
- [22] Mao J M and Delos J B 1992 *Phys. Rev. A* **45** 1746
- [23] Poston T and Stewart I N 1978 *Catastrophe Theory and Its Applications* (London: Pitman)
- [24] Bleistein N and Handelsman R A 1986 *Asymptotic Expansions of Integrals* (New York: Dover)
- [25] Kuś M, Haake F and Delande D 1993 *Phys. Rev. Lett.* **71** 2167